

ARTICLE



Loss of exosomal miR-200b-3p from hypoxia cancer-associated fibroblasts promotes tumorigenesis and reduces sensitivity to 5-Flourouracil in colorectal cancer via upregulation of ZEB1 and E2F3

Wenjing Gong^{1,2}, Yang Guo^{1,2}, Hang Yuan^{1,2}, Rui Chai¹, Ziang Wan¹, Boan Zheng¹, Xinye Hu¹, Bingchen Chen¹, Shan Gao¹, Qiaoqiong Dai¹, Peng Yu¹ and Shiliang Tu¹

© The Author(s), under exclusive licence to Springer Nature America, Inc. 2023

Hypoxia-mediated tumor progression is a major clinical challenge in human cancers including colorectal cancer (CRC). In addition, exosome-mediated transfer of miRNAs from cancer-associated fibroblasts (CAFs) to cancer cells could promote tumor progression. However, the mechanisms by which hypoxia CAFs promotes CRC progression remain largely unknown. CAFs and normal fibroblasts (NFs) were isolated from CRC tissues and adjacent normal tissues. Next, exosomes were isolated from the supernatant of CAFs that cultured under normoxia (CAFs-N-Exo) and hypoxia (CAFs-H-Exo). RNA-sequencing was then performed to identify differentially expressed miRNAs (DEMs) between CAFs-N-Exo and CAFs-H-Exo. Compared with exosomes derived from normoxia CAFs, exosomes derived from hypoxic CAFs were able to promote CRC cell proliferation, migration, invasion, stemness and reduce the sensitivity of CRC cells to 5-fluorouracil (5-FU). In addition, miR-200b-3p levels were dramatically decreased in exosomes derived from hypoxic CAFs. Remarkably, increasing exosomal miR-200b-3p in hypoxic CAFs reversed the promoting effects of hypoxic CAFs on CRC cell growth in vitro and in vivo. Furthermore, miR-200b-3p agomir could inhibit CRC cell migration, invasion, stemness and increase the sensitivity of SW480 cells to 5-FU via downregulating ZEB1 and E2F3. Collectively, loss of exosomal miR-200b-3p in hypoxia CAFs could contribute to CRC progression via upregulation of ZEB1 and E2F3. Thus, increasing exosomal miR-200b-3p might serve as an alternative approach for the treatment of CRC.

Cancer Gene Therapy (2023) 30:905–916; <https://doi.org/10.1038/s41417-023-00591-5>

INTRODUCTION

Colorectal cancer (CRC) is known as the third most common malignancy worldwide with substantial incidence and mortality [1, 2]. Although surgical resection and adjuvant therapies including chemotherapy, immunotherapy and radiotherapy have been used to treat CRC, the overall 5-year survival rate of patients with metastatic CRC remains less than 15% [3–5]. In addition, difficulty in early diagnosis and aggressive local metastasis formation are the primary causes of high mortality in patients with CRC [6, 7]. Thus, identifying new diagnostic biomarkers and understanding of the biological mechanisms of CRC may improve early diagnosis and treatment of CRC.

Hypoxic tumor microenvironment (TME), a common phenomenon in solid tumors, is closely related to chemoresistance, increased invasion and metastasis in cancers [8–10]. Hypoxia can contribute to the aggressive tumor behaviors and facilitate distant metastasis [11, 12]. In addition, tumor cells may adapt to hypoxic TME mainly via upregulating the hypoxia-inducible factor-1 α (HIF-1 α) [13]. Significantly, HIF-1 α promoted tumor cell survival, invasion, angiogenesis via activating a set of genes [14–16].

Cancer-associated fibroblasts (CAFs) are the major cellular components in the TME, which could promote cancer progression and chemoresistance [17–19]. It has been shown that hypoxic cancer cells could promote the activation of CAFs, leading to increased invasion and stemness of cancer cells [20]. In addition, hypoxic CAFs could promote endothelial cell angiogenesis [21]. In particular, the communication between CAFs and surrounding cells are often mediated by exosomes [22]. Exosomes (40–150 nm) contain different nucleic acids including microRNAs (miRNAs) that could mediate communication between CAFs and cancer cells [23–25]. Hu et al. found that exosomal miR-92a-3p released from CAFs could promote CRC cell metastasis and chemotherapy resistance [26]. However, the mechanisms by which hypoxic CAFs promote CRC cell invasion, stemness and chemotherapy resistance remain unclear. In this study, we found that miR-200b-3p level was significantly decreased in hypoxic CAFs-derived exosomes (CAFs-H-Exo). In addition, CAFs-H-Exo could enhance CRC cell migration, invasion, stemness and reduce the sensitivity of CRC cells to the chemotherapeutic agent 5-fluorouracil (5-FU); whereas these phenomena were abolished by exosomes

¹General Surgery, Cancer Center, Department of Colorectal Surgery, Zhejiang Provincial People's Hospital (Affiliated People's Hospital, Hangzhou Medical College), Hangzhou, Zhejiang 310014, PR China. ²These authors contributed equally: Wenjing Gong, Yang Guo, Hang Yuan. email: tushiliang@hmc.edu.cn

Received: 8 August 2022 Revised: 5 January 2023 Accepted: 17 January 2023

Published online: 8 March 2023

containing miR-200b-3p agomir. Thus, increasing exosomal miR-200b-3p might serve as an alternative approach for the treatment of CRC.

MATERIALS AND METHODS

Clinical samples

A total of 5 pairs of CRC tissues and paired normal tissues were collected from the patients undergoing a surgical procedure at the Zhejiang Provincial People's Hospital. Next, primary CAFs and NFs were isolated from tumor tissues and adjacent normal tissues, as previously described [27]. This study was approved by the Ethics Committee of Zhejiang Provincial People's Hospital, and the written informed consent was obtained from each participant.

Cell culture and cell transfection

CAFs and NFs were maintained in DMEM/F12 medium containing 10% FBS at 37 °C with 5% CO₂. For hypoxia stimulation, CAFs were cultured in a hypoxia chamber with 1% O₂ for 24 h.

In addition, human colon normal cell line CCD 841 CoN, human CRC cell lines HCT116, SW620 and SW480 were obtained from the American Type Culture Collection (ATCC) and maintained in DMEM (Thermo Fisher Scientific) medium containing 10% FBS at 37 °C with 5% CO₂. These cell lines were tested negative for mycoplasma contamination and authenticated by STR profiling.

MiR-200b-3p agomir, miR-200b-3p antagomir and negative control (NC) plasmids were obtained from RIBOBIO. Meanwhile, HIF-1 α , ZEB1 or E2F3 was ligated into the pcDNA3.1 vector to obtain pcDNA3.1-HIF-1 α (HIF-1 α OE), pcDNA3.1-ZEB1 (ZEB1 OE) or pcDNA3.1-E2F3 (E2F3 OE) plasmids (GenePharma). Cells were transfected with indicated plasmids above using Lipofectamine 2000.

Reverse transcription quantitative real-time polymerase chain reaction (RT-qPCR)

Total RNA was extracted using the TRIpure Total RNA Extraction Reagent (ELK Biotechnology) and then reverse-transcribed into cDNA using the EntiLink™ 1st Strand cDNA Synthesis Kit (ELK Biotechnology). Next, qPCR was conducted on the StepOne™ Real-Time PCR System with the EnTurbo™ SYBR Green PCR SuperMix kit (ELK Biotechnology). MiR-200b-3p expression was normalized to U6 and E2F3 and ZEB1 levels were normalized to β -actin using the 2^{- $\Delta\Delta$ Ct} method. The information of primers was provided in Table 1.

Immunofluorescence (IF) assay

CAFs and NFs were washed with PBS, fixed with 4% paraformaldehyde for 20 min and then blocked in 1% BSA for 30 min. After that, cells were incubated overnight at 4 °C with a primary antibody against α -SMA (Abcam), followed by incubation with a secondary antibody conjugated with fluorescent Alexa Fluor® 594 (Abcam) for 1 h in darkness. Finally, cells were visualized using a fluorescence microscope. Nuclei were stained with DAPI for 10 min.

Table 1. The information of primers.

Name		Primer sequences (5'-3')
miR-200b-3p	Forward	GGCCCTAATACTGCCTGGTA
	Reverse	CTCAACTGGTGTCTGGAGTC
U6	Forward	CTCGCTTCGGCAGCACAT
	Reverse	AACGCTTCACGAATTTGCGT
E2F3	Forward	AAGGAAGAGCTGCACTACGAAG
	Reverse	GCTGCCTTGTCAAATCCAAT
ZEB1	Forward	GAATCATCGCTACTCCTACTGTAAG
	Reverse	CTCTTTTCACTGTCTTCATCCTCT
β -actin	Forward	GTCCACCGCAAATGCTTCTA
	Reverse	TGCTGTACCTTACCGTTC

Western blot assay

Protein concentrations were determined using a bicinchoninic acid (BCA) kit (Beyotime). After that, proteins were electrophoresed on 10% SDS-PAGE and then transferred to a PVDF membrane. The membrane was then incubated with primary antibodies against α -SMA (1:1000, cat. no. AF1032, Affinity Biosciences), FAP (1:1000, cat. no. AF0739, Affinity Biosciences), CD9 (1:5000, cat. no. 60232-1-Ig, Proteintech), CD81 (1:2000, cat. no. 66866-1-Ig, Proteintech), HSP70 (1:2000, cat. no. 25405-1-AP, Proteintech), HIF-1 α (1:2000, cat. no. 20960-1-AP, Proteintech), CD133 (1:1000, cat. no. 18470-1-AP, Proteintech), SOX2 (1:2000, cat. no. 66411-1-Ig, Proteintech), β -actin (1:1000, cat. no. 66009-1-Ig, Proteintech), ZEB1 (1:2000, cat. no. 66279-1-Ig, Proteintech), E2F3 (1:500, cat. no. 27615-1-AP, Proteintech), E-cadherin (1:2000, cat. no. 20874-1-AP, Proteintech), N-cadherin (1:2000, cat. no. 22018-1-AP, Proteintech), cyclin E1 (1:1000, AF0144, Affinity Biosciences), CDK2 (1:2000, cat. no. 10122-1-AP, Proteintech), p21 (1:2000, cat. no. 10355-1-AP, Proteintech), calnexin (1:1000, cat. no. 10427-2-AP, Proteintech) and GAPDH (1:10000, cat. no. ab181602, Abcam) overnight at 4 °C, followed by incubation with appropriate secondary antibodies for 1 h at room temperature. Next, an enhanced chemiluminescence kit (Thermo Fisher Scientific) was used for protein detection.

Exosome isolation and identification

CAFs were cultured under normoxic or hypoxic conditions (CAFs-N and CAFs-H). Exosomes were purified from CAFs-N (CAFs-N-Exo) or CAFs-H (CAFs-H-Exo) by ultracentrifugation, as previously described [28]. After that, exosomes were resuspended in 100 μ L of PBS.

For nanoparticle tracking analysis (NTA), size distributions of exosomes were determined using a ZetaView nanoparticle tracking analyzer (Particle Metrix).

For transmission electron microscopy (TEM) assay, exosomes were fixed in 2.5% glutaraldehyde, loaded on a carbon-coated copper grid, and then stained with 1% phosphotungstic acid. After that, morphologies of exosomes were observed by a transmission electron microscope.

RNA-sequencing

Total RNA was extracted from CAFs-N-Exo and CAFs-H-Exo using TRIpure Total RNA Extraction Reagent (ELK Biotechnology). Next, the QIAseq miRNA Library Kit was used to construct the RNA-seq libraries. After that, the libraries were sequenced by Illumina HiSeq sequencer (Illumina). Limma package of R software was used to analyze the DEMs between CRC tissues and paired normal tissues [29]. DEMs were obtained with $|\log_2(\text{fold change})| > 1$ and adjusted p value < 0.05 .

Gene ontology (GO, <http://www.geneontology.org/>) was used to predict the possible functions of the target genes of DEMs and Kyoto Encyclopedia of Genes and Genomes (KEGG, <http://www.genome.jp/kegg/>) enrichment analysis were performed to predict the potential pathways that the target genes of DEMs may participate in.

Exosome uptake

CAFs-N-Exo and CAFs-H-Exo were stained for 30 min with PKH26 dye (Sigma). Next, the PKH26-labeled exosomes (red color) were co-cultured with SW480 cells for 24 h. After that, the uptake of exosomes in SW480 cells were observed by a confocal microscope.

Co-culture system

CAFs-N and CAFs-H were transfected with Cy3-labeled miR-200b-3p. Next, the transfected CAFs-N or CAFs-H cells were plated onto a Transwell® polyester permeable supports. Meanwhile, SW480 cells were seeded onto a bottom chamber. SW480 cells (bottom chamber) were co-cultured with transfected CAFs-N or CAFs-H cells (upper chamber) for 48 h. Subsequently, SW480 cells were observed using a confocal microscope.

Cell-counting Kit-8 (CCK-8) assay

SW480 and HCT116 cells were seeded onto 96-well plates (5000 cells/well) overnight at 37 °C. After that, each well was added with 10 μ L of CCK-8 reagent (Beyotime). After 2 h of incubation, absorbance was measured by a microplate reader at the wavelength of 450 nm.

EdU staining assay

The Cell-light EdU DNA Cell Proliferation kit (RiboBio) was used to detect cell proliferation. Briefly, SW480 cells were incubated with EdU reagent for 30 min and then stained with Apollo dye solution for 30 min in darkness.

After that, cells were stained with Hoechst 33342 for 30 min in darkness. Next, a fluorescence microscope was applied to observe the EdU-positive cells.

TdT-mediated dUTP nick end labeling (TUNEL) assay

The In Situ Cell Death Detection Kit (Roche) was applied to assess cell apoptosis. SW480 cells were treated with 4% paraformaldehyde, then stained with the TUNEL reaction mixture in darkness at 37 °C for 1 h. Subsequently, the apoptotic cells were observed by a fluorescence microscope.

Transwell assays

Cell migration and invasion abilities were measured with Transwell assays using 24-well Transwell chambers (Corning). SW480 and HCT116 cells suspended in 100 µL of serum-free DMEM medium were plated onto the upper chamber, and 500 µL of DMEM medium plus 10% FBS were added into the lower chamber. After 24 h of incubation, cells that passed through the filter were stained with 0.2% crystal violet. Subsequently, the migratory or invasive cells were observed using a light microscope. For the invasion assay, the upper chamber was pre-coated with matrigel (BD Bioscience).

Sphere-forming assay

SW480 cells (2000 cells/ml) were grown on an ultra-low attachment 6-well plate (Corning) and cultured in sphere medium (DMEM/F12 medium plus 20 ng/ml EGF, 10 ng/ml FGF, 4 ng/ml insulin and 2% B27), and incubated for 14 days at 37 °C. Later on, cells were captured using a light microscopy.

Luciferase reporter assay

The wild-type or mutant 3' UTR of ZEB1 and E2F3 was inserted into the pGL6-miR-based luciferase reporter vector (Beyotime). After that, SW480 cells were co-transfected with indicated pGL6-miR-based reporter plasmids and miR-200b-3p using Lipofectamine 2000 for 48 h. Subsequently, the luciferase activity was detected in cell lysates using the Dual Luciferase Reporter Assay System (Promega).

Animal study

Four-week-old male BALB/c nude mice were obtained from Youdu Biotech (Wuhan, China). SW480 cells (10^7 cells) were subcutaneously injected into left flank of nude mice. When the tumors reach about 200 mm³ in size, animals were divided randomly into 4 groups ($n = 6$): control, CAFs-N-NC-Exo, CAFs-H/NC-Exo, and CAFs-H/miR-200b-3p agomir-Exo groups. Next, PBS, CAFs-N-NC-Exo, CAFs-H/NC-Exo, and CAFs-H/miR-200b-3p agomir-Exo was injected intratumorally twice weekly for 3 weeks. Tumor volume was calculated by the following formula: $(\text{length} \times \text{width}^2)/2$. After that, the mice were euthanized at day 21, and then the tumor tissues were dissected out. Next, tumor volume and tumor weight were measured. Cell apoptosis in tumor tissues was determined by the APO-BrdU™ TUNEL Assay Kit. Animal study was approved by the ethics committee of the Zhejiang Provincial People's Hospital and animals were maintained following the institutional guidelines. The sample size used in this study was based on the experience in previous research. The investigator was blinded to the group allocation.

Immunohistochemistry (IHC) assay

Tumor tissues were paraffin-embedded and then cut into 3 µm sections. After that, sections were incubated overnight at 4 °C with the primary antibodies against CD133 and N-cadherin, followed by incubation with horseradish peroxidase conjugated anti-rabbit second antibody for 30 min. Subsequently, sections were visualized by using DAB solution, counterstained with haematoxylin, and then observed using a light microscope.

Statistical analyses

Experiments were repeated in triplicate. Data are expressed as the mean ± standard deviation (S.D.). Group comparisons were analyzed by One-way analysis of variance (ANOVA) and Tukey's tests. Differences between two group were analyzed using paired Student's *t*-test. An estimate of variation within each group of data was conducted. The differences were considered significant at * $P < 0.05$.

RESULTS

Identification of DEMs between CAFs-N-Exo and CAFs-H-Exo

It has been shown that tumor cell growth is closely related to TME in which hypoxia and CAFs are two major factors [30, 31]. Therefore, to better understand the communication between CRC cells and hypoxic CAFs, CAFs and NFs were isolated from CRC tissues and paired normal tissues respectively. As shown in Fig. 1A, B, compared with NFs, the expressions of the specific fibroblast markers α -SMA and FAP were much higher in CAFs, suggesting that CAFs were isolated successfully. Next, exosomes (CAFs-N-Exo and CAFs-H-Exo) were collected from the conditioned medium (CM) of CAFs that cultured under normoxia and hypoxia respectively. These two vesicles were identified as round and cup-shaped membrane-coated particles with a range of 40 to 150 nm in diameter (Fig. 1C, D). In addition, these two vesicles expressed exosomal markers CD9, CD81 and HSP70, whereas the endoplasmic reticulum protein calnexin was negative expressed in these two vesicles (Supplementary Fig. 1). These data showed that these vesicles were exosomes.

To explore how CAFs-H-Exo exert their effects on CRC cells, RNA sequencing was used to screen DEMs between CAFs-N-Exo and CAFs-H-Exo. The results revealed that 21 downregulated miRNAs (including miR-200b-3p) were detected in CAFs-H-Exo compared to CAFs-N-Exo (Fig. 1F, G). In addition, GO results revealed that the target genes of these 21 DEMs were mainly enriched in the category "protein binding" (Supplementary Fig. 2A). KEGG pathway analysis showed that the target genes of these 21 DEMs were mainly involved in "pathways in cancer" pathway (Supplementary Fig. 2B).

MiR-200 family plays an important role in cancer development and acts as diagnostic and prognostic biomarkers for various cancers [32, 33]. MiR-200b-3p, a member of miR-200 family, can act as a tumor suppressor in human cancers including CRC [34, 35]. In addition, the data from starbase database (<http://starbase.sysu.edu.cn/index.php>) showed that low miR-200b-3p level was associated with worse overall survival rates in patients with CRC (Fig. 1H). Meanwhile, the level of miR-200b-3p was significantly downregulated in CRC tissues and CRC cell lines (HCT116, SW620 and SW480) (Fig. 1I, J). Furthermore, miR-200b-3p levels was markedly reduced in CAFs-H and CAFs-H-Exo compared to CAFs-N and CAFs-N-Exo respectively (Fig. 1K). Collectively, miR-200b-3p level was decreased in hypoxic CAFs and hypoxic CAFs-derived exosomes.

HIF-1 α inhibited the level of miR-200b-3p in hypoxic CAFs

In the abovementioned experiments, we found that hypoxia could decrease miR-200b-3p level in CAFs compared to normoxia condition. It has been shown that HIF-1 α , an active transcription factor in the hypoxic TME, could regulate the expressions of miRNAs [36, 37]. Therefore, we focus on investigating the correlation between miR-200b-3p and HIF-1 α in hypoxic CAFs. As shown in Fig. 2A, the expression of HIF-1 α was significantly increased in hypoxic CAFs compared with that in normoxic CAFs. In addition, the expression of HIF-1 α was notably upregulated in CAFs transfected with HIF-1 α OE plasmids (Fig. 2B). Subsequent experiments showed that overexpression of HIF-1 α remarkably reduced miR-200b-3p level in CAFs under hypoxic condition (Fig. 2C). These data showed that HIF-1 α could decrease miR-200b-3p level in hypoxic CAFs.

Hypoxic CAFs-derived exosomes transferred miR-200b-3p into SW480 cells

To investigate whether miR-200b-3p could be transfer from hypoxic CAFs to CRCs via exosomes, SW480 cells were incubated with PKH26-labeled CAFs-N-Exo or PKH26-labeled CAFs-H-Exo. As shown in Fig. 3A, PKH26 dye was observed in CAFs-N-Exo and CAFs-H-Exo-treated SW480 cells. In addition, SW480 cells were co-cultured with normoxic or hypoxic CAFs that were

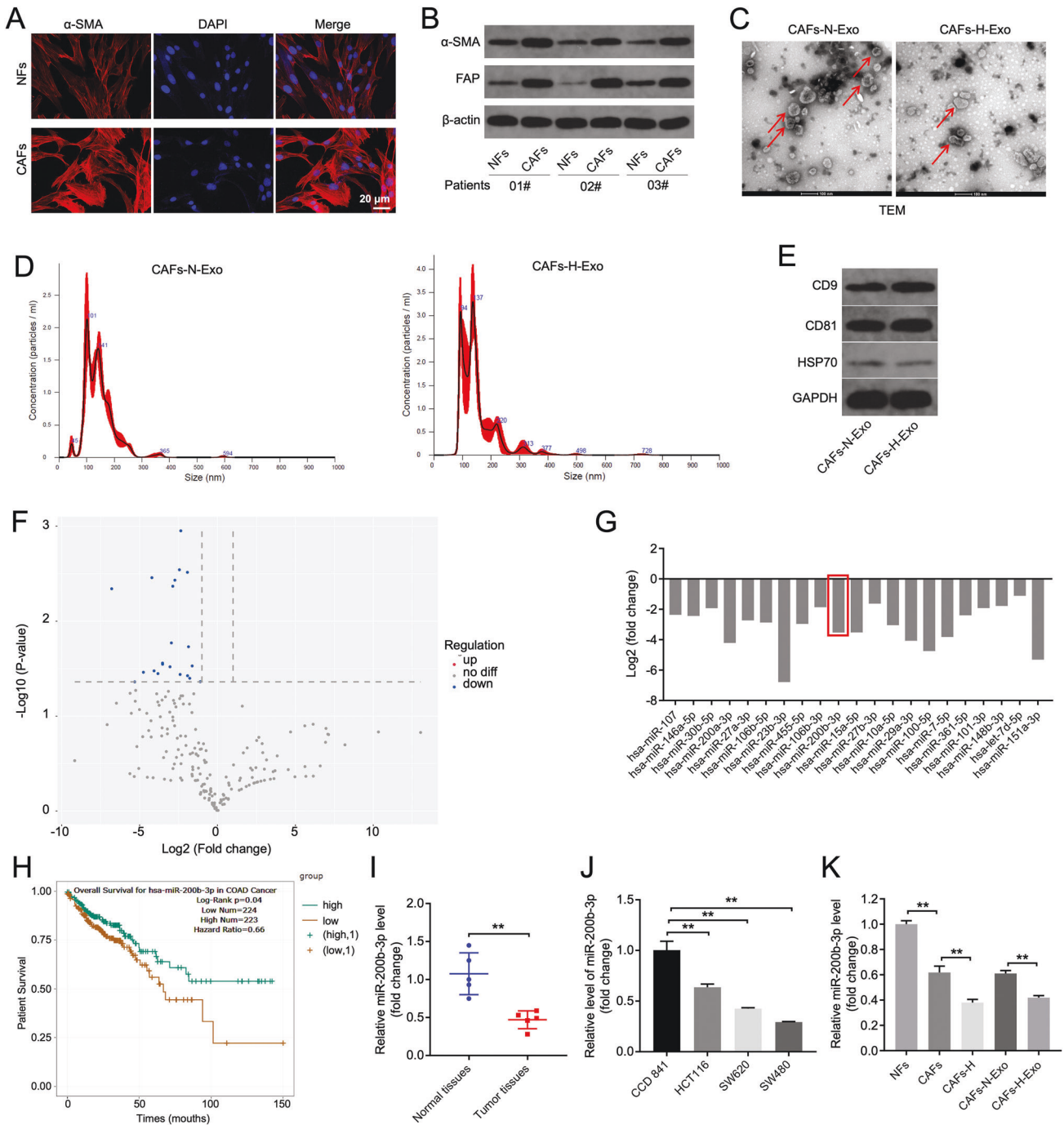


Fig. 1 Identification of DEMs between CAFs-N-Exo and CAFs-H-Exo. **A** IF staining for α -SMA expression in CAFs and NFs. **B** Western blot analysis of α -SMA and FAP expressions in three paired CAFs and NFs. **C, D** Identification of exosomes (CAF-N-Exo and CAF-H-Exo) derived from CAFs that cultured under normoxia and hypoxia by TEM and NTA analysis. Red arrow points at exosomes. **E** Western blot analysis of CD9, CD81 and HSP70 in CAFs-N-Exo and CAFs-H-Exo. **F** Volcano plot of DEMs between CAFs-N-Exo and CAFs-H-Exo. **G** 21 downregulated miRNAs between CAFs-N-Exo and CAFs-H-Exo were identified using R language. **H** Survival analysis revealed the relation between overall survival rate and the level of miR-200b-3p in patients with CRC in Starbase database. **I** RT-qPCR analysis of miR-200b-3p level in 5 paired CRC tissues and matched normal tissues. **J** RT-qPCR analysis of miR-200b-3p levels in HCT116, SW620 and SW480 cells. **K** RT-qPCR analysis of miR-200b-3p level in CAFs-N, CAFs-H, CAFs-N-Exo, and CAFs-H-Exo. ****** $P < 0.01$.

transfected with Cy3-labeled miR-200b-3p agomir. The results showed that Cy3 fluorescence dye was observed in SW480 cells as well (Fig. 3B). To sum up, miR-200b-3p is contained in normoxic or hypoxic CAFs-secreted exosomes and can be transferred to SW480 cells.

Next, we explored the existing pattern of extracellular miR-200b-3p. As shown in Fig. 3C, combination of RNase A and Triton X-100 remarkably reduced miR-200b-3p level in the CM of hypoxic or normoxic CAFs compared to RNase A treatment group, indicating that extracellular miR-200b-3p was encased by the membrane.

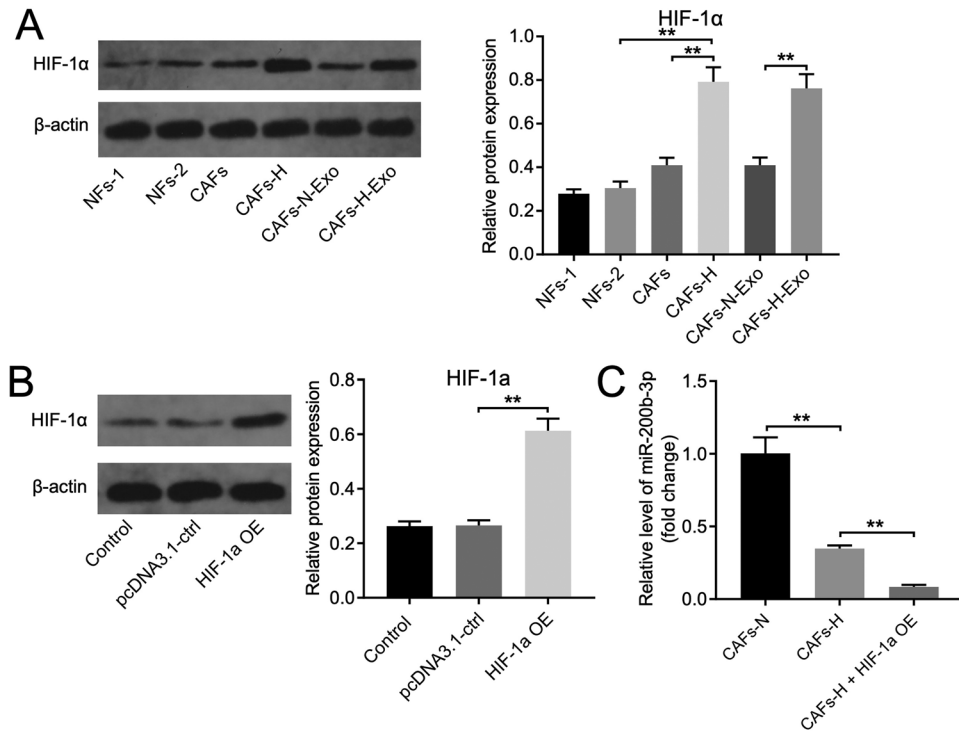


Fig. 2 HIF-1 α inhibited miR-200b-3p level in hypoxic CAFs. **A** Western blot analysis of HIF-1 α protein expression in CAFs-N, CAFs-H, CAFs-N-Exo and CAFs-H-Exo. **B** Western blot analysis of HIF-1 α protein expression in CAFs transfected with HIF-1 α OE plasmids. **C** RT-qPCR analysis was used to measure miR-200b-3p level in hypoxia CAFs and hypoxia CAFs transfected with HIF-1 α OE plasmids. ****** $P < 0.01$.

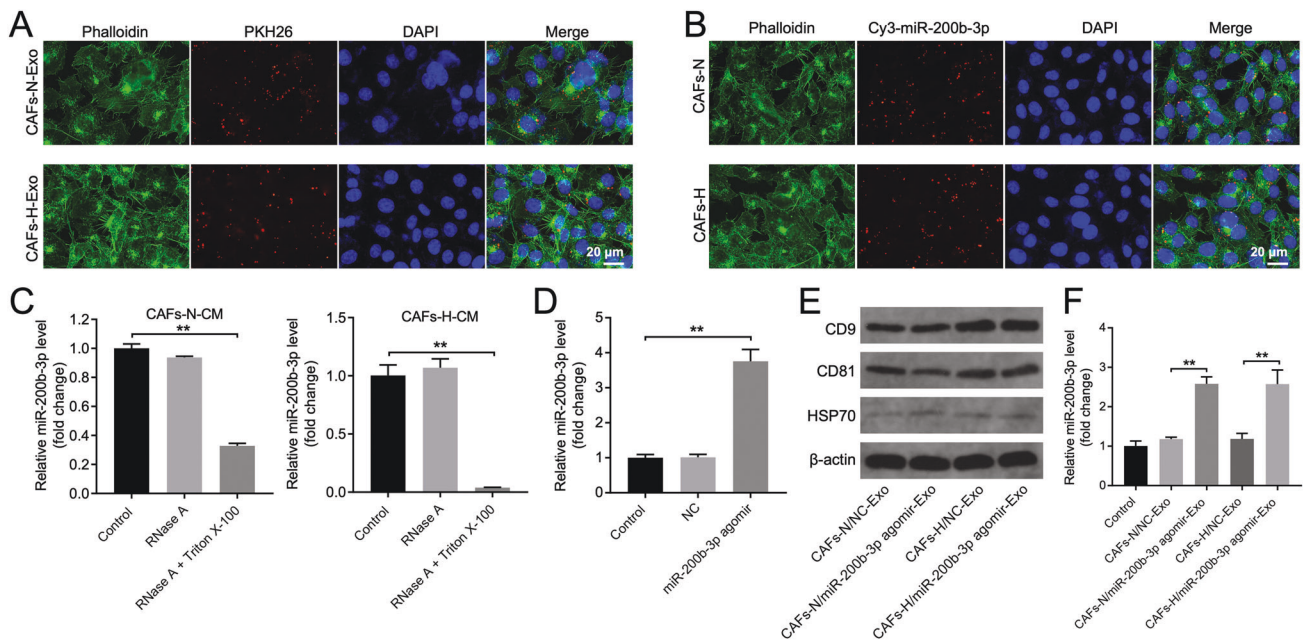


Fig. 3 Hypoxic CAFs exosomes transferred miR-200b-3p into SW480 cells. **A** Immunofluorescence images showed the internalization of PKH26-labeled CAFs-N-Exo or CAFs-H-Exo (red) by SW480 cells. **B** CAFs-N or CAFs-H transfected with Cy3-labeled miR-200b-3p were co-cultured with SW480 cells. Fluorescence microscopy was used to detect Cy3 signals (red) in SW480 cells. **C** The culture supernatants were collected from CAFs that cultured under normoxia and hypoxia. RT-qPCR analysis of miR-200b-3p level in culture supernatants treated with RNase A alone or combined with Triton X-100. **D** RT-qPCR analysis of miR-200b-3p level in CAFs transfected with NC or miR-200b-3p agomir. **E** Western blot analysis of exosome surface markers CD9, CD81 and HSP70 in indicated exosomes. **F** RT-qPCR analysis of miR-200b-3p level in SW480 cells after incubation with indicated exosomes. ****** $P < 0.01$.

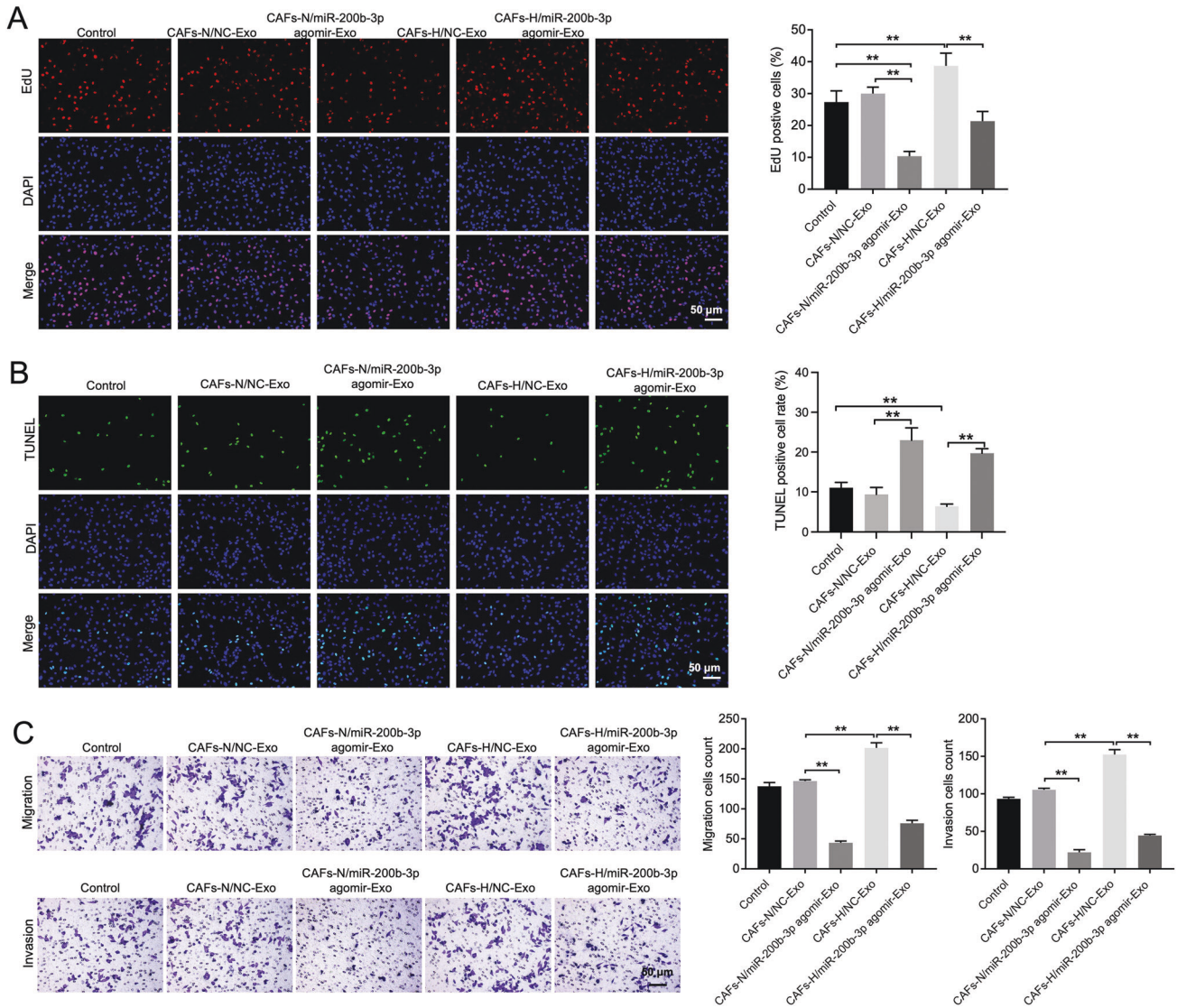


Fig. 4 Loss of miR-200b-3p in hypoxic CAFs-derived exosomes promoted SW480 cell proliferation, migration, invasion. SW480 cells were treated with indicated exosomes for 48 h. **A** EdU and **B** TUNEL staining assays were conducted to measure cell proliferation and apoptosis. **C** SW480 cells were treated with indicated exosomes for 24 h. Transwell assays were used to determine cell migration and invasion. ****** $P < 0.01$.

In addition, the level of miR-200b-3p was remarkably increased in CAFs transfected with miR-200b-3p agomir (Fig. 3D). Meanwhile, exosomes were isolated from normoxic (CAFs-N/NC-Exo and CAFs-N/miR-200b-3p agomir-Exo) or hypoxic CAFs (CAFs-H/NC-Exo, and CAFs-H/miR-200b-3p agomir-Exo) that were transfected with NC or miR-200b-3p agomir. Western blot results showed that these isolated vesicles expressed exosomal markers CD9, CD81 and HSP70, suggesting that these vesicles were exosomes (Fig. 3E). Additionally, the level of miR-200b-3p was notably increased in SW480 cells incubated with CAFs-N/miR-200b-3p agomir-Exo and CAFs-H/miR-200b-3p agomir-Exo compared to SW480 cells incubated with CAFs-N/NC-Exo and CAFs-H/NC-Exo (Fig. 3F). Collectively, miR-200b-3p can be transferred from hypoxic CAFs to SW480 cells via exosomes.

Loss of miR-200b-3p in hypoxic CAFs-derived exosomes promoted CRC cell proliferation, migration, invasion, stemness and reduced the sensitivity of CRC cells to 5-FU

Next, we focused on investigating the role of miR-200b-3p in the interaction between hypoxic CAFs and SW480 cells. As revealed in

Fig. 4A–C and Supplementary Fig. 3A, CAFs-H/NC-Exo remarkably enhanced the viability, proliferation, migration, and invasion of SW480 cells and significantly reduced SW480 cell apoptosis compared to control or CAFs-N/NC-Exo group, whereas these changes were notably abolished by hypoxic CAFs-derived exosomes containing miR-200b-3p agomir. In contrast, compared to CAFs-N/NC-Exo group, hypoxic CAFs-derived exosomes containing miR-200b-3p antagonist further promoted HCT116 cell viability, migration, and invasion (Supplementary Fig. 3B–E).

Furthermore, CAFs-H/NC-Exo markedly elevated the sphere-forming efficiency and increased the expressions of stemness markers CD133 and SOX2 in SW480 cells compared to control or CAFs-N/NC-Exo group, whereas these phenomena were reversed by CAFs-H/miR-200b-3p agomir-Exo (Fig. 5A, B). Moreover, CCK-8 and EdU staining assays showed that CAFs-H/NC-Exo significantly reduced the sensitivity of SW480 cells to 5-FU; however, these changes were notably reversed by CAFs-H/miR-200b-3p agomir-Exo (Fig. 5C, D). To sum up, loss of miR-200b-3p in CAFs-H-Exo could enhance CRC cell proliferation, migration, invasion, stemness and reduce the sensitivity of CRC cells to 5-FU.

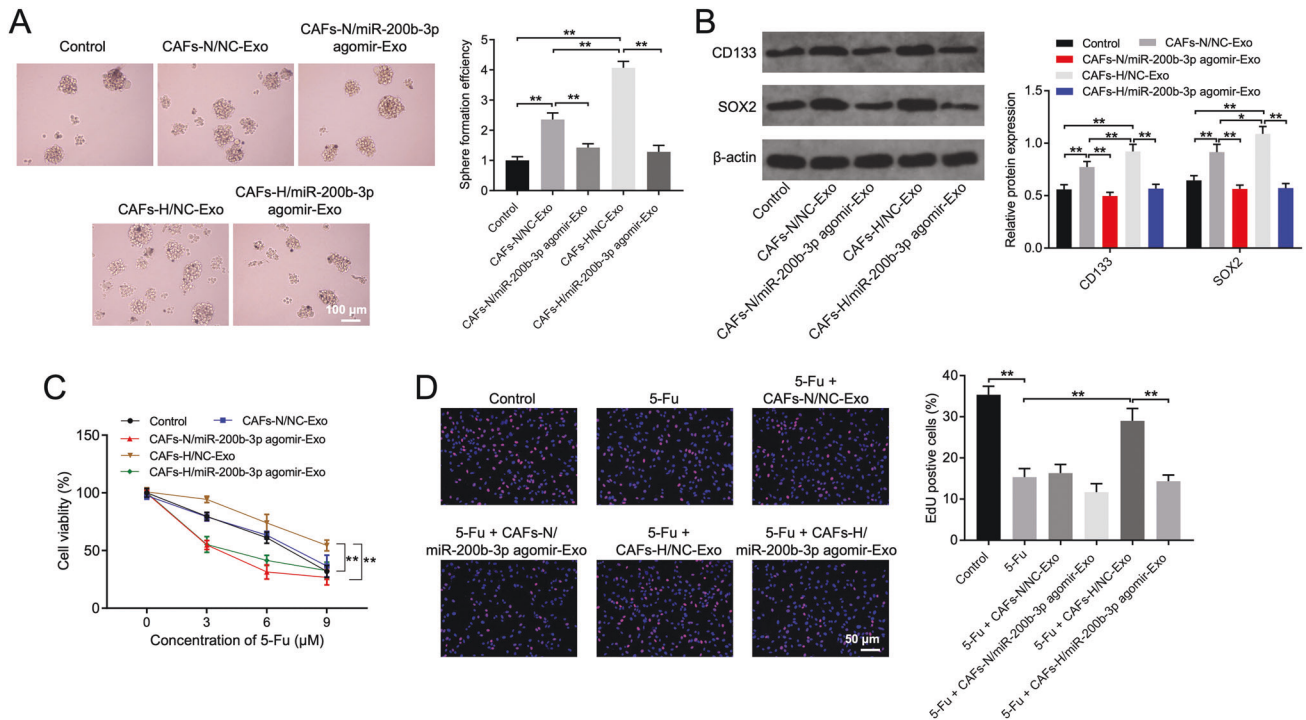


Fig. 5 Loss of miR-200b-3p in hypoxic CAFs-derived exosomes promoted SW480 cell stemness and reduced the sensitivity of CRC cells to 5-FU. **A** SW480 cells were treated with indicated exosomes. Sphere forming assay was applied to determine the self-renewal of the CRC cells. **B** Western blot was applied to determine CD133 and SOX2 protein expressions in SW480 cells. **C, D** SW480 cells were treated with indicated exosomes for 48 h, followed by 5-FU treatment for 72 h. CCK-8 and EdU staining assay was used to measure cell viability and proliferation. * $P < 0.05$, ** $P < 0.01$.

ZEB1 and E2F3 were direct targets of exosomal miR-200b-3p in CRC

It has been shown that miRNAs could affect disease development via regulating target gene expressions [38, 39]. Therefore, TargetScan database was used to predict the downstream targets of miR-200b-3p. The data showed that ZEB1 and E2F3 might be potential targets of miR-200b-3p (Fig. 6A). Furthermore, the results of dual-luciferase reporter assay demonstrated that the luciferase activity of 3' UTR of ZEB1-wild type or E2F3-wild type was reduced by miR-200b-3p agomir, indicating that miR-200b-3p could directly target ZEB1 and E2F3 (Fig. 6B).

In addition, the expression of ZEB1 or E2F3 was markedly upregulated in SW480 cells transfected with ZEB1 OE or E2F3 OE plasmids respectively (Fig. 6C). Moreover, miR-200b-3p agomir significantly reduced the levels of ZEB1 and E2F3 in SW480 cells; whereas ZEB1 or E2F3 overexpression dramatically increased ZEB1 or E2F3 level in SW480 cells (Fig. 6D, E). Meanwhile, CAFs-H/NC-Exo notably increased the expressions of ZEB1 and E2F3 in SW480 cells compared to control or CAFs-N/NC-Exo group (Fig. 6E). These results indicated that ZEB1 and E2F3 were direct targets of exosomal miR-200b-3p in CRC.

MiR-200b-3p inhibited SW480 cell proliferation, migration, invasion, stemness and increased the sensitivity of SW480 cells to 5-FU via targeting ZEB1 and E2F3

After identifying ZEB1 and E2F3 as direct targets of miR-200b-3p, we then investigated whether miR-200b-3p could regulate SW480 cell growth via targeting ZEB1 and E2F3. As indicated in Fig. 7A, overexpression of miR-200b-3p markedly suppressed SW480 cell migration and invasion, whereas these changes were reversed by ZEB1 or E2F3 overexpression. In addition, CCK-8 assay results revealed that miR-200b-3p agomir dramatically enhanced the sensitivity of CRC cells to 5-FU, whereas

these changes were reversed by ZEB1 or E2F3 overexpression (Fig. 7B). Moreover, miR-200b-3p agomir markedly inhibited the sphere-forming efficiency of SW480 cells; however, that change was reversed by ZEB1 or E2F3 overexpression (Fig. 7C). Furthermore, miR-200b-3p agomir significantly reduced the expressions of CD133, SOX2 and N-cadherin and increased the expression of E-cadherin in SW480 cells, whereas these changes were reversed by ZEB1 overexpression (Fig. 7D). Meanwhile, overexpression of miR-200b-3p notably decreased the expressions of Cyclin E1 and CDK2 and increased the expression of p21, whereas these changes were reversed by E2F3 overexpression (Fig. 7E). Collectively, miR-200b-3p could inhibit SW480 cell proliferation, migration, invasion, stemness and increase the sensitivity of SW480 cells to 5-FU via downregulating ZEB1 and E2F3.

Loss of miR-200b-3p in hypoxic CAFs-derived exosomes promoted SW480 cell growth and stemness in vivo

Finally, we investigated the effect of CAFs-H-Exo on the tumorigenicity of CRC in vivo. As shown in Fig. 8A, B, CAFs-H/NC-Exo markedly promoted the tumor volume and tumor weight of SW480 subcutaneous xenografts compared with control and CAFs-N/NC-Exo group, whereas these phenomena were reversed by CAFs-H/miR-200b-3p agomir-Exo. Additionally, CAFs-H/NC-Exo notably decreased miR-200b-3p level in tumor tissues compared with control and CAFs-N/NC-Exo group; however, that change was increased by CAFs-H/miR-200b-3p agomir-Exo (Fig. 8C). Moreover, CAFs-H/NC-Exo remarkably inhibited cell apoptosis in tumor tissues, whereas that effect was reversed by CAFs-H/miR-200b-3p agomir-Exo (Fig. 8D). Meanwhile, CAFs-H/NC-Exo significantly upregulated the expressions of CD133, N-cadherin, ZEB1 and E2F3 in tumor tissues, whereas these phenomena were reversed by CAFs-H/miR-200b-3p agomir-Exo

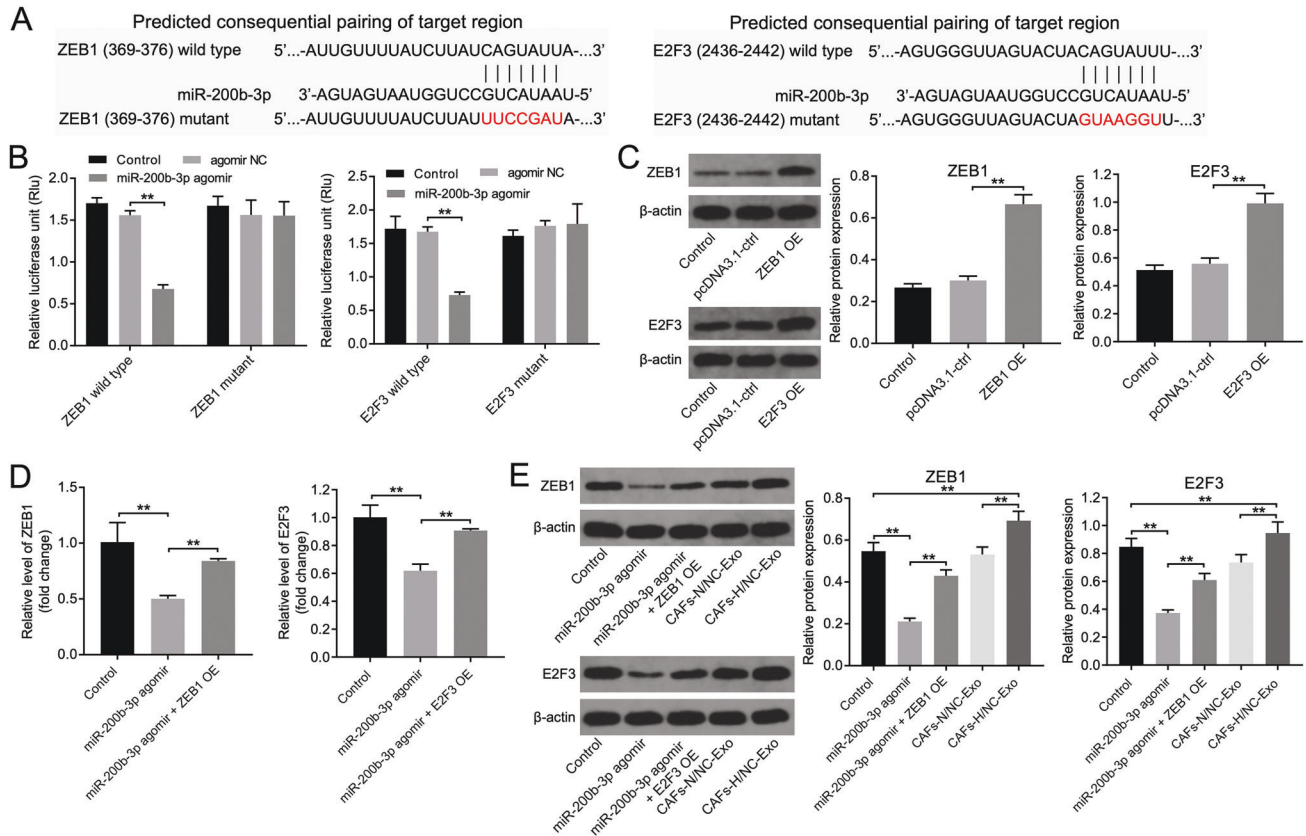


Fig. 6 ZEB1 and E2F3 were direct targets of exosomal miR-200b-3p in CRC. **A** The complementary sequences or mutant binding sites between ZEB1 and miR-200b-3p, and between E2F3 and miR-200b-3p. **B** Luciferase activity analysis in SW480 cells treated with the ZEB1/E2F3-wild type/mutant plasmids together with miR-200b-3p agomir. **C** SW480 cells were treated with ZEB1 OE or E2F3 OE plasmids respectively. Western blot analysis of ZEB1 or E2F3 protein expression in transfected SW480 cells. **D** SW480 cells were treated with miR-200b-3p agomir or miR-200b-3p agomir plus ZEB1 or E2F3 plasmids respectively. RT-qPCR analysis of ZEB1 or E2F3 level in transfected SW480 cells. **E** SW480 cells were treated with miR-200b-3p agomir, miR-200b-3p agomir plus ZEB1 or E2F3 plasmids or indicated exosomes respectively. Western blot analysis of ZEB1 or E2F3 protein expression in SW480 cells. ** $P < 0.01$.

(Fig. 8E, F). These data showed that loss of miR-200b-3p in hypoxic CAFs-derived exosomes could promote SW480 cell growth and stemness in vivo.

DISCUSSION

Hypoxia is a key microenvironmental factor promoting tumor survival and progression [40]. In addition, CAFs are a major cellular component of TME in most cancers, which could affect cancer progression via promoting tumor cell growth, angiogenesis and extracellular matrix remodeling [41, 42]. In this study, we focused on the communication between hypoxic CAFs and CRC cells. Recently, exosomes have emerged as important mediators for cell-to-cell communication through transporting miRNAs [43]. Li et al. found that CAFs-derived exosomal miR-34a-5p promoted the proliferation and metastasis of oral squamous cell carcinoma cells [44]. In addition, Xia et al. found that hypoxic gastric cancer-derived exosomal miR-301a-3p could promote gastric cancer malignant behaviors and metastasis [45]. However, the effect of hypoxia on CAFs has not been extensively investigated. Our results found that hypoxic CAFs-derived exosomes could enhance the migration, invasion, stemness of CRC cells and reduced the sensitivity of CRC cells to 5-FU, compared to normoxic CAFs-derived exosomes. Our research firstly explored the role of hypoxic CAFs-derived exosomes in CRC. Increasing evidence demonstrated that exosome-mediated transfer of miRNAs from CAFs to tumor

cells could promote cancer progression and chemoresistance [43, 46]. In this study, we found that the level of miR-200b-3p was significantly decreased in hypoxic CAFs-derived exosomes compared with that in normoxic CAFs-derived exosomes. Importantly, miR-200b-3p could be transferred from hypoxic CAFs to CRC cells via exosomes. Next, to investigate the role of exosomal miR-200b-3p in tumorigenesis, we isolated exosomes from hypoxic CAFs transfected with miR-200b-3p agomir. Our results found that hypoxic CAFs-derived exosomes could promote the migration, invasion, stemness of CRC cells and reduced the sensitivity of CRC cells to 5-FU, whereas these phenomena were reversed by hypoxic CAFs-derived exosomes with high miR-200b-3p expression. These data showed that increasing exosomal miR-200b-3p in hypoxic CAFs could reverse the promoting effects of hypoxic CAFs on CRC cell growth. Meanwhile, exosomal miR-200b-3p plays an important role in the TME interactions and is vital for tumor growth in CRC.

Furthermore, ZEB1 and E2F3 were verified as downstream targets of miR-200b-3p in CRC. ZEB1, an inducer for epithelial-mesenchymal transition (EMT) in human cancers, was able to promote tumor invasion and drug resistance [47, 48]. Goulet et al. found that CAFs could induce EMT phenotype in bladder cancer cells via upregulation of ZEB1 [49]. Additionally, E2F3 is an important cell cycle regulator that promotes tumor cell proliferation, EMT, invasion and chemoresistance [50–52]. Feng et al. showed that downregulation of miR-200b was able to

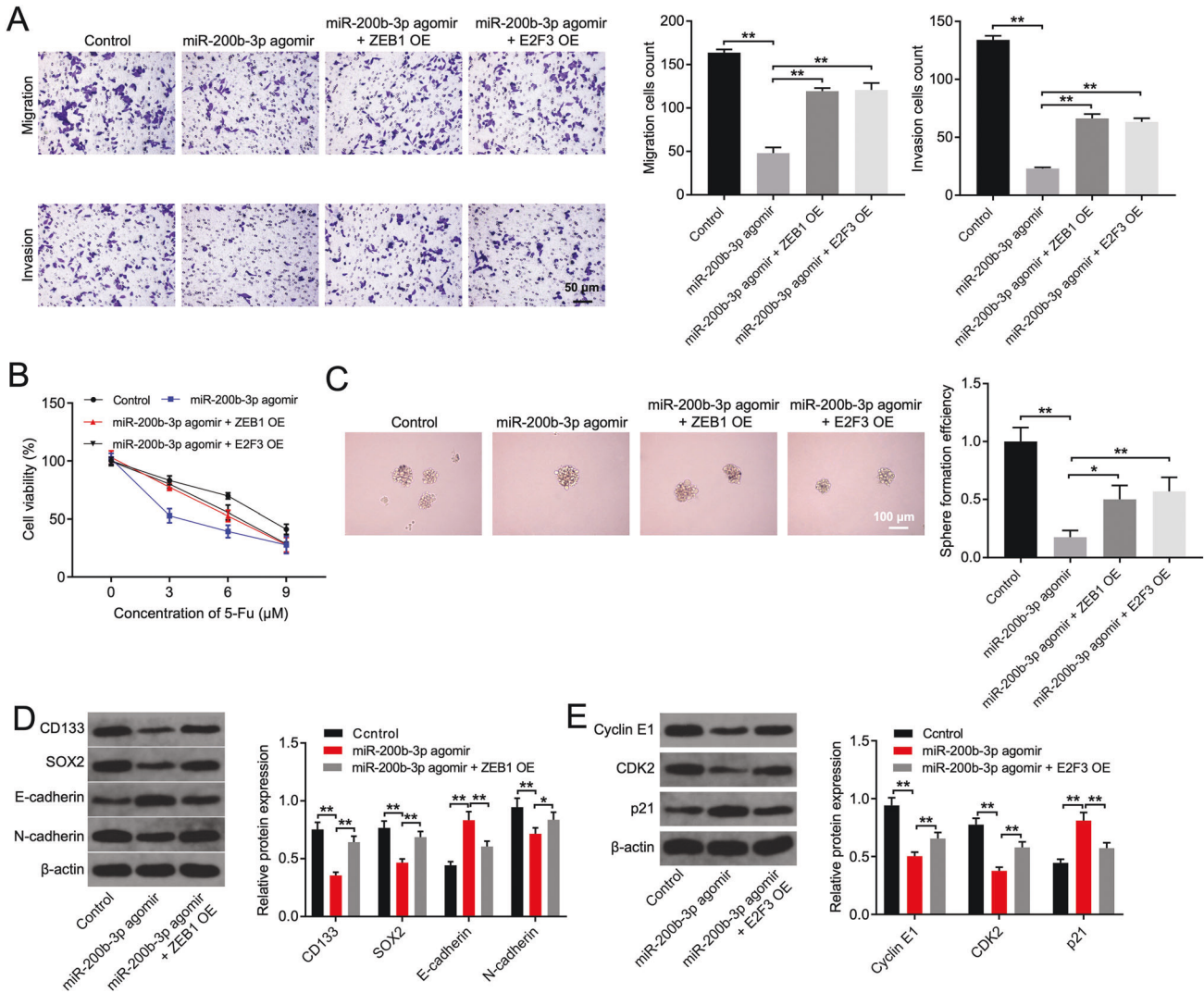


Fig. 7 MiR-200b-3p inhibited SW480 cell proliferation, migration, invasion, stemness and increased the sensitivity of SW480 cells to 5-FU via targeting ZEB1 and E2F3. **A** SW480 cells were treated with miR-200b-3p agomir or miR-200b-3p agomir plus ZEB1 or E2F3 plasmids respectively. Transwell assays were used to determine cell migration and invasion. **B** SW480 cells were treated with miR-200b-3p agomir or miR-200b-3p agomir plus ZEB1 or E2F3 plasmids respectively, followed by 5-FU treatment for 72 h. CCK-8 assay was applied to determine cell viability. **C** SW480 cells were treated with miR-200b-3p agomir or miR-200b-3p agomir plus ZEB1 or E2F3 plasmids respectively. Sphere forming assay was applied to determine the self-renewal of the CRC cells. **D** SW480 cells were treated with miR-200b-3p agomir or miR-200b-3p agomir plus ZEB1 plasmids. Western blot analysis of CD133, SOX2, E-cadherin and N-cadherin protein expressions in transfected SW480 cells. **E** SW480 cells were treated with miR-200b-3p agomir or miR-200b-3p agomir plus E2F3 plasmids. Western blot analysis of cyclin E1, CDK2 and p21 protein expressions in transfected SW480 cells. * $P < 0.05$, ** $P < 0.01$.

promote the chemoresistance of lung cancer cells to docetaxel via upregulation of E2F3 [53]. Here, we found that miR-200b-3p obviously inhibited CRC cell proliferation, migration, invasion and increased the sensitivity of CRC cells to 5-FU, whereas overexpression of ZEB1 or E2F3 reversed these changes. Furthermore, compared to CAFs-N/NC-Exo, CAFs-H/NC-Exo notably decreased the level of miR-200b-3p, and elevated the expressions of ZEB1 and E2F3 in SW480 cells. Collectively, loss of miR-200b-3p in hypoxic CAFs-derived exosomes could promote SW480 cell proliferation, migration, invasion, stemness and reduced the sensitivity of CRC cells to 5-FU via upregulation of ZEB1 and E2F3.

Indeed, there are some limitations in this study. First, our results found that exosomes derived from hypoxic CAFs could increase the sphere-forming efficiency in CRC cells. Evidence has shown that hypoxia can be appeared in the core of larger spheroids [54].

Thus, we plan to investigate whether exosomes derived from hypoxic CAFs could affect hypoxic-core formation in spheroids CRC cells in the future. Second, CAFs-derived exosomes could facilitate the metastasis of CRC [26]. However, the effect of hypoxic CAFs-derived exosomes on tumor metastasis in CRC remains largely unclear. Thus, further studies are needed to explore the effect of CAFs-H/miR-200b-3p agomir-Exo on metastasis in CRC in vivo.

CONCLUSION

Our results revealed that loss of exosomal miR-200b-3p from hypoxia CAFs could promote CRC progression via upregulation of ZEB1 and E2F3. Thus, increasing exosomal miR-200b-3p might serve as an alternative approach for the treatment of CRC.

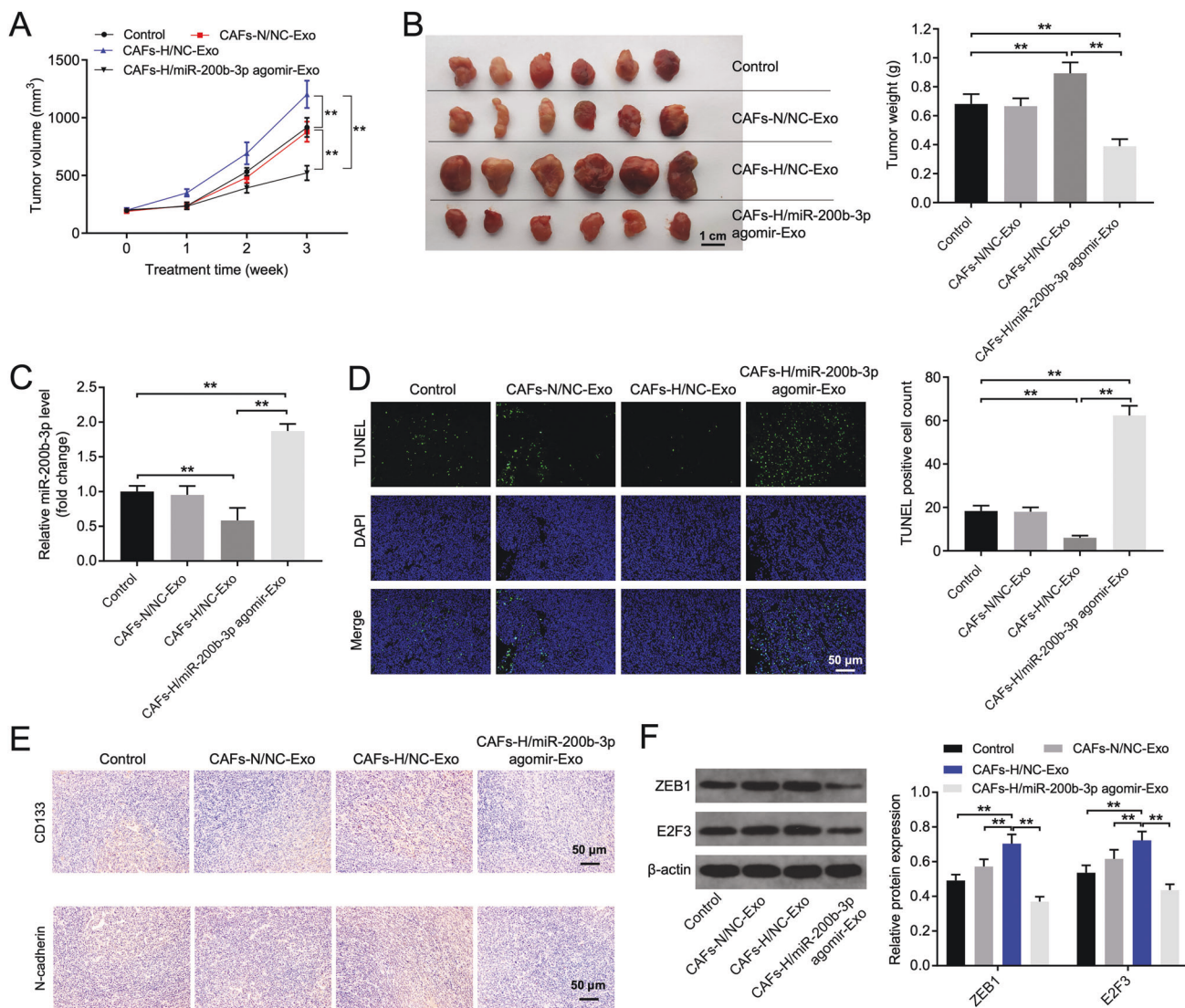


Fig. 8 Loss of miR-200b-3p in hypoxic CAFs-derived exosomes promoted SW480 cell growth and stemness in vivo. **A, B** Tumor volume and tumor weight of xenograft tumors. **C** RT-qPCR analysis of miR-200b-3p level in tumor tissues. **D** TUNEL analysis of cell apoptosis in tumor tissues. **E** IHC analysis of CD133 and N-cadherin protein expressions in tumor tissues. **F** Western blot analysis of ZEB1 and E2F3 protein expressions in tumor tissues. ****** $P < 0.01$.

DATA AVAILABILITY

The datasets used and/or analyzed during the current study are available from the corresponding author on reasonable request.

REFERENCES

- Balacescu O, Sur D, Cainap C, Visan S, Cruceriu D, Manzat-Saplan R. The Impact of miRNA in Colorectal Cancer Progression and Its Liver Metastases. *Int J Mol Sci*. 2018;19:3711.
- Wang L, Cho KB, Li Y, Tao G, Xie Z, Guo B. Long Noncoding RNA (lncRNA)-Mediated Competing Endogenous RNA Networks Provide Novel Potential Biomarkers and Therapeutic Targets for Colorectal Cancer. *Int J Mol Sci*. 2019;20:5758.
- Piawah S, Venook AP. Targeted therapy for colorectal cancer metastases: A review of current methods of molecularly targeted therapy and the use of tumor biomarkers in the treatment of metastatic colorectal cancer. *Cancer*. 2019;125:4139–47.
- Kuipers EJ, Grady WM, Lieberman D, Seufferlein T, Sung JJ, Boelens PG, et al. Colorectal cancer. *Nat Rev Dis Prim*. 2015;1:15065.
- Bashir B, Snook AE. Immunotherapy regimens for metastatic colorectal carcinomas. *Hum Vaccin Immunother*. 2018;14:250–4.
- Sousa-Squiavinato ACM, Vasconcelos RI, Gehren AS, Fernandes PV, de Oliveira IM, Boroni M, et al. Cofilin-1, LIMK1 and SSH1 are differentially expressed in locally advanced colorectal cancer and according to consensus molecular subtypes. *Cancer cell Int*. 2021;21:69.
- Aguirre-Portolés C, Feliu J, Reglero G, Ramírez de Molina A. ABCA1 overexpression worsens colorectal cancer prognosis by facilitating tumour growth and caveolin-1-dependent invasiveness, and these effects can be ameliorated using the BET inhibitor apabetalone. *Mol Oncol*. 2018;12:1735–52.
- McKeown SR. Defining normoxia, physoxia and hypoxia in tumours-implications for treatment response. *Br J Radiol*. 2014;87:20130676.
- Krishnamachary B, Mironchik Y, Jacob D, Goggins E, Kakkad S, Ofori F, et al. Hypoxia theranostics of a human prostate cancer xenograft and the resulting effects on the tumor microenvironment. *Neoplasia*. 2020;22:679–88.
- Meng W, Hao Y, He C, Li L, Zhu G. Exosome-orchestrated hypoxic tumor microenvironment. *Mol Cancer*. 2019;18:57.
- Silvoniemi A, Sulamo S, Laitinen T, Forsback S, Löyttyniemi E, Vaittinen S, et al. Repeatability of tumour hypoxia imaging using [(18)F]EF5 PET/CT in head and neck cancer. *Eur J Nucl Med Mol imaging*. 2018;45:161–9.
- Qin Y, Liu HJ, Li M, Zhai DH, Tang YH, Yang L, et al. Salidroside improves the hypoxic tumor microenvironment and reverses the drug resistance of platinum drugs via HIF-1 α signaling pathway. *EBioMedicine*. 2018;38:25–36.

13. Ni J, Wang X, Stojanovic A, Zhang Q, Wincher M, Bühler L, et al. Single-Cell RNA Sequencing of Tumor-Infiltrating NK Cells Reveals that Inhibition of Transcription Factor HIF-1 α Unleashes NK Cell Activity. *Immunity*. 2020;52:1075–1087.
14. Campbell EJ, Dachs GU, Morrin HR, Davey VC, Robinson BA, Vissers MCM. Activation of the hypoxia pathway in breast cancer tissue and patient survival are inversely associated with tumor ascorbate levels. *BMC Cancer*. 2019;19:307.
15. Garg N, Kumar P, Gadhawe K, Giri R. The dark proteome of cancer: Intrinsic disorder and functionality of HIF-1 α along with its interacting proteins. *Prog Mol Biol Transl Sci*. 2019;166:371–403.
16. De Francesco EM, Lappano R, Santolla MF, Marsico S, Caruso A, Maggiolini M. HIF-1 α /GPER signaling mediates the expression of VEGF induced by hypoxia in breast cancer associated fibroblasts (CAFs). *Breast Cancer Res*. 2013;15:R64.
17. Wu HJ, Hao M, Yeo SK, Guan JL. FAK signaling in cancer-associated fibroblasts promotes breast cancer cell migration and metastasis by exosomal miRNAs-mediated intercellular communication. *Oncogene*. 2020;39:2539–49.
18. Sazeides C, Le A. Metabolic Relationship between Cancer-Associated Fibroblasts and Cancer Cells. *Adv Exp Med Biol*. 2018;1063:149–65.
19. Su S, Chen J, Yao H, Liu J, Yu S, Lao L, et al. CD10(+)/GPR77(+) Cancer-Associated Fibroblasts Promote Cancer Formation and Chemoresistance by Sustaining Cancer Stemness. *Cell*. 2018;172:841–856.e16.
20. Deep G, Panigrahi GK. Hypoxia-Induced Signaling Promotes Prostate Cancer Progression: Exosomes Role as Messenger of Hypoxic Response in Tumor Microenvironment. *Crit Rev Oncog*. 2015;20:419–34.
21. Kugeratski FG, Atkinson SJ, Neilson LJ, Lilla S, Knight JRP, Serneels J. Hypoxic cancer-associated fibroblasts increase NCBP2-AS2/HIAR to promote endothelial sprouting through enhanced VEGF signaling. *Sci Signal*. 2019;12:eaan8247.
22. Wang H, Wei H, Wang J, Li L, Chen A, Li Z. MicroRNA-181d-5p-Containing Exosomes Derived from CAFs Promote EMT by Regulating CDX2/HOXA5 in Breast Cancer. *Mol Ther Nucleic Acids*. 2020;19:654–67.
23. Ge Q, Zhou Y, Lu J, Bai Y, Xie X, Lu Z. miRNA in plasma exosome is stable under different storage conditions. *Molecules*. 2014;19:1568–75.
24. Richards KE, Zeleniak AE, Fishel ML, Wu J, Littlepage LE, Hill R. Cancer-associated fibroblast exosomes regulate survival and proliferation of pancreatic cancer cells. *Oncogene*. 2017;36:1770–8.
25. Kalluri R. The biology and function of exosomes in cancer. *J Clin Investig*. 2016;126:1208–15.
26. Hu JL, Wang W, Lan XL, Zeng ZC, Liang YS, Yan YR, et al. CAFs secreted exosomes promote metastasis and chemotherapy resistance by enhancing cell stemness and epithelial-mesenchymal transition in colorectal cancer. *Mol Cancer*. 2019;18:91.
27. Li YY, Zhou CX, Gao Y. Interaction between oral squamous cell carcinoma cells and fibroblasts through TGF- β 1 mediated by podoplanin. *Exp Cell Res*. 2018;369:43–53.
28. Zeng Z, Li Y, Pan Y, Lan X, Song F, Sun J, et al. Cancer-derived exosomal miR-25-3p promotes pre-metastatic niche formation by inducing vascular permeability and angiogenesis. *Nat Commun*. 2018;9:5395.
29. Ritchie ME, Phipson B, Wu D, Hu Y, Law CW, Shi W, et al. limma powers differential expression analyses for RNA-sequencing and microarray studies. *Nucleic Acids Res*. 2015;43:e47.
30. Wanandi SI, Ningsih SS, Asikin H, Hosea R, Neolaka GMG. Metabolic Interplay between Tumour Cells and Cancer-Associated Fibroblasts (CAFs) under Hypoxia versus Normoxia. *Malays J Med Sci*. 2018;25:7–16.
31. Petrova V, Annicchiarico-Petruzzelli M, Melino G, Amelio I. The hypoxic tumour microenvironment. *Oncogenesis*. 2018;7:10.
32. Huang GL, Sun J, Lu Y, Liu Y, Cao H, Zhang H, et al. MiR-200 family and cancer: From a meta-analysis view. *Mol Asp Med*. 2019;70:57–71.
33. Cavallari I, Ciccarese F, Sharova E, Urso L, Raimondi V, Silic-Benusi M, et al. The miR-200 Family of microRNAs: Fine Tuners of Epithelial-Mesenchymal Transition and Circulating. *Cancer Biomarkers*. 2021;13:5874.
34. Chen L, Wang X, Zhu Y, Zhu J, Lai Q. miR-200b-3p inhibits proliferation and induces apoptosis in colorectal cancer by targeting Wnt1. *Mol Med Rep*. 2018;18:2571–80.
35. Wu J, Cui H, Zhu Z, Wang L. MicroRNA-200b-3p suppresses epithelial-mesenchymal transition and inhibits tumor growth of glioma through down-regulation of ERK5. *Biochem Biophys Res Commun*. 2016;478:1158–64.
36. Karshovska E, Wei Y, Subramanian P, Mohibullah R, Geißler C, Baatsch I, et al. HIF-1 α (Hypoxia-Inducible Factor-1 α) Promotes Macrophage Necroptosis by Regulating miR-210 and miR-383. *Arterioscler Thromb Vasc Biol*. 2020;40:583–96.
37. Wu L, Chen Y, Chen Y, Yang W, Han Y, Lu L, et al. Effect of HIF-1 α /miR-10b-5p/PTEN on Hypoxia-Induced Cardiomyocyte Apoptosis. *J Am Heart Assoc*. 2019;8:e011948.
38. Tutar Y. miRNA and cancer; computational and experimental approaches. *Curr Pharm Biotechnol*. 2014;15:429.
39. Ferragut Cardoso AP, Udoh KT, States JC. Arsenic-induced changes in miRNA expression in cancer and other diseases. *Toxicol Appl Pharmacol*. 2020;409:115306.
40. Noman MZ, Messai Y, Carré T, Akalay I, Méron M, Janji B, et al. Microenvironmental hypoxia orchestrating the cell stroma cross talk, tumor progression and antitumor response. *Crit Rev Immunol*. 2011;31:357–77.
41. Zhao H, Yang L, Baddour J, Achreja A, Bernard V, Moss T, et al. Tumor micro-environment derived exosomes pleiotropically modulate cancer cell metabolism. *eLife*. 2016;5:e10250.
42. Monteran L, Erez N. The Dark Side of Fibroblasts: Cancer-Associated Fibroblasts as Mediators of Immunosuppression in the Tumor Microenvironment. *Front Immunol*. 2019;10:1835.
43. Yang F, Yan Y, Yang Y, Hong X, Wang M, Yang Z, et al. MiR-210 in exosomes derived from CAFs promotes non-small cell lung cancer migration and invasion through PTEN/PI3K/AKT pathway. *Cell Signal*. 2020;73:109675.
44. Li YY, Tao YW, Gao S, Li P, Zheng JM, Zhang SE, et al. Cancer-associated fibroblasts contribute to oral cancer cells proliferation and metastasis via exosome-mediated paracrine miR-34a-5p. *EBioMedicine*. 2018;36:209–20.
45. Xia X, Wang S, Ni B, Xing S, Cao H, Zhang Z, et al. Hypoxic gastric cancer-derived exosomes promote progression and metastasis via MiR-301a-3p/PHD3/HIF-1 α positive feedback loop. *Oncogene*. 2020;39:6231–44.
46. Qin X, Guo H, Wang X, Zhu X, Yan M, Wang X, et al. Exosomal miR-196a derived from cancer-associated fibroblasts confers cisplatin resistance in head and neck cancer through targeting CDKN1B and ING5. *Genome Biol*. 2019;20:12.
47. Richard G, Dalle S, Monet MA, Ligier M, Boespflug A, Pommier RM, et al. ZEB1-mediated melanoma cell plasticity enhances resistance to MAPK inhibitors. *EMBO Mol Med*. 2016;8:1143–61.
48. Cortés M, Sanchez-Moral L, de Barrios O, Fernández-Aceñero MJ, Martínez-Campanario MC, Esteve-Codina A, et al. Tumor-associated macrophages (TAMs) depend on ZEB1 for their cancer-promoting roles. *EMBO J*. 2017;36:3336–55.
49. Goulet CR, Champagne A, Bernard G, Vandal D, Chabaud S, Pouliot F, et al. Cancer-associated fibroblasts induce epithelial-mesenchymal transition of bladder cancer cells through paracrine IL-6 signalling. *BMC Cancer*. 2019;19:137.
50. Ma M, Wang X, Chen X, Cai R, Chen F, Dong W, et al. MicroRNA-432 targeting E2F3 and P53PIK inhibits myogenesis through PI3K/AKT/mTOR signaling pathway. *RNA Biol*. 2017;14:347–60.
51. Jusino S, Rivera-Rivera Y, Chardón-Colón C, Ruiz-Justiz AJ, Vélez-Velázquez J, Isidro A, et al. E2F3 drives the epithelial-to-mesenchymal transition, cell invasion, and metastasis in breast cancer. *Exp Biol Med*. 2021;246:2057–71.
52. Wu QB, Sheng X, Zhang N, Yang MW, Wang F. Role of microRNAs in the resistance of colorectal cancer to chemoradiotherapy. *Mol Clin Oncol*. 2018;8:523–7.
53. Feng B, Wang R, Song HZ, Chen LB. MicroRNA-200b reverses chemoresistance of docetaxel-resistant human lung adenocarcinoma cells by targeting E2F3. *Cancer*. 2012;118:3365–76.
54. Voissiere A, Jouberton E, Maubert E, Degoul F, Peyrode C, Chezal JM, et al. Development and characterization of a human three-dimensional chondrosarcoma culture for in vitro drug testing. *PLoS One*. 2017;12:e0181340.

AUTHOR CONTRIBUTIONS

WG, YG and HY carried out experiments and made major contributions to the design and manuscript drafting of this study. RC, ZW, BZ, XH, BC, SG, QD and PY were responsible for investigation, data analysis, data interpretation. ST conceived experiments and revised the manuscript critically for important intellectual content. All authors agreed to be accountable for all aspects of the work. All authors read and approved the final manuscript.

FUNDING

The present study was financially supported by the Natural Science Foundation of Zhejiang Province (LY18H160041, LY17H160064, LQ21H160042), the Funding Project of Health and Family Planning Commission of Zhejiang Province (2018KY217), and the Funding Project Administration of Traditional Chinese Medicine of Zhejiang Province (2018ZA009).

COMPETING INTERESTS

The authors declare no competing interests.

ETHICS APPROVAL AND CONSENT TO PARTICIPATE

All procedures were approved by the ethics committee of the Zhejiang Provincial People's Hospital.

ADDITIONAL INFORMATION

Supplementary information The online version contains supplementary material available at <https://doi.org/10.1038/s41417-023-00591-5>.

Correspondence and requests for materials should be addressed to Shiliang Tu.

Reprints and permission information is available at <http://www.nature.com/reprints>

Publisher's note Springer Nature remains neutral with regard to jurisdictional claims in published maps and institutional affiliations.

Springer Nature or its licensor (e.g. a society or other partner) holds exclusive rights to this article under a publishing agreement with the author(s) or other rightsholder(s); author self-archiving of the accepted manuscript version of this article is solely governed by the terms of such publishing agreement and applicable law.